A modular sound-attenuating metasurface with subwavelength thickness and hexagonal unit cells

Alexandru Crivoi and Zheng Fan

Citation: Proc. Mtgs. Acoust. **39**, 040002 (2019); doi: 10.1121/2.0001288
View online: https://doi.org/10.1121/2.0001288
View Table of Contents: https://asa.scitation.org/toc/pma/39/1
Published by the Acoustical Society of America

Volume 39 http://acousticalsociety.org/

178th Meeting of the Acoustical Society of America
San Diego, CA
2-6 December 2019

Noise: Paper 1pSA16

A modular sound-attenuating metasurface with subwavelength thickness and hexagonal unit cells

Alexandru Crivoi and Zheng Fan
School of Mechanical and Aerospace Engineering, Nanyang Technological University, Singapore, 639798, SINGAPORE; acrivoi@ntu.edu.sg; zfan@ntu.edu.sg

A sound attenuating subwavelength metamaterial efficient in the low audible frequency range is proposed. The metasurface unit cell has a hexagonal shape with an axial ventilation channel inside. The side walls of the hexagonal cell are sub-divided into six hollow chambers connected to the central air path via the six thinner channels of different diameters. The hollow chambers act as Helmholtz resonators providing six different resonant frequencies for each cell. The negative effective bulk modulus property of the metasurface allows near-full sound block at the resonant frequencies and partial sound adsorption inside the intermediate frequency bands. By carefully designing the size of the connecting side holes we can adjust the desired sound attenuation frequency range. The thickness of the metasurface is in the range of 0.05–0.15 wavelengths for the sound frequency range between 300 and 1000 Hz. The hexagonal shape of the unit cell allows full honeycomb tessellation of the metasurface volume. By designing a hybrid metasurface containing individual cells with different resonators, the absorption peaks can be multiplied or merged together thus further broadening the frequency range with the transmission coefficient lower than the desired threshold value.

Published by the Acoustical Society of America

 https://doi.org/10.1121/2.0001288

1. INTRODUCTION

The noise attenuation problem has a long history and has traditionally been linked to the industrial environment with a heavy machinery. However, in the recent decades, increasing urban population density and vehicle traffic has led to the high demand for low cost noise cancelling solutions in the residential areas. In Singapore, the combination of hot tropical climate and high levels of noise pollution have created a strong demand for environmental noise-reducing metasurfaces covering a broad range of audible frequencies and having a designated pathway for the air ventilation.

Sound attenuation is usually achieved by implementation of sound barrier structures which operate on either sound absorption or sound reflection principle. However, in the low audible frequency range (250-500 Hz), such barriers might be bulky and challenging to install in the residential areas. Some earlier applications of duct acoustics have managed to produce sound attenuation with the preserved ventilation capacity,[1–5] most notable of which are Herschel-Quincke waveguides.[6] These solutions usually have a large physical footprint and narrow-band absorption capacity. More recent development saw the implementation of metamaterials for the noise reduction applications.[7–9] A notable recent paper featured a metasurface with Fano-like interference to achieve a significant sound attenuation in a low frequency range while preserving a large ratio of the ventilation duct cross-section.[9] Another recent attempts focused on sound absorption by using coiled space with perforated plates,[10] Faubrey-Perot (FP) resonance in channels,[11] Double Fishnet (DF) plates[12] and coupled Helmholtz resonators.[13,14] However, the main challenge has been to produce a simple, easy-to-manufacture meta-structure which can be mass-produced and satisfactorily perform in a broad frequency range of audible noise.

In this paper, we present a sound barrier design with sub-wavelength thickness based on multiple coupled Helmholtz resonators, allowing a high ventilation area ratio and flexible range of target peak absorption frequencies.

2. DESIGN AND MODELLING

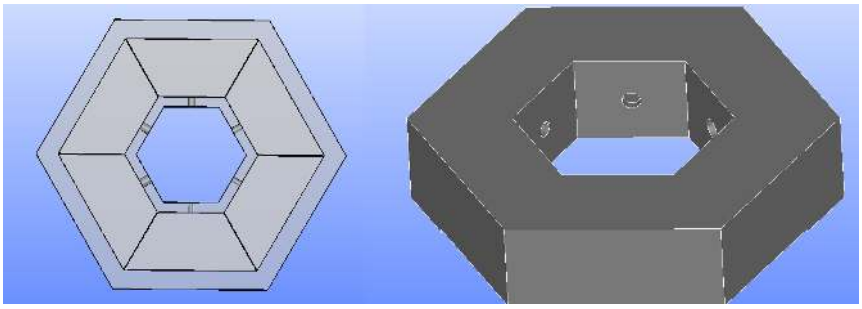

Figure 1: Design of the metasurface hexagonal unit cell. (left) normal 2D schematic of the cell indicating six inner cavities of equal volume, (right) isometric 3D view of the cell.

Figure 1 shows the geometry of unit hexagonal cell. The inner volume of the cell is sub-divided into six hollow chambers connected to the central duct via the six cylindrical pathways of different diameters. The hollow chambers act as Helmholtz resonators providing six different resonant frequencies for each cell. The negative effective bulk modulus property of the cell allows full sound absorption at the resonant frequencies. By carefully choosing the diameters of the connecting channels we can manipulate the desired sound adsorption frequency range. The thickness of the sound barrier composed of such cells is in the range of 0.03-0.1 wavelengths for the audible sound frequency range between 300 and 1000 Hz.

The design process of the hexagonal cell has been automated using the Salome CAD/CAE platform[15]

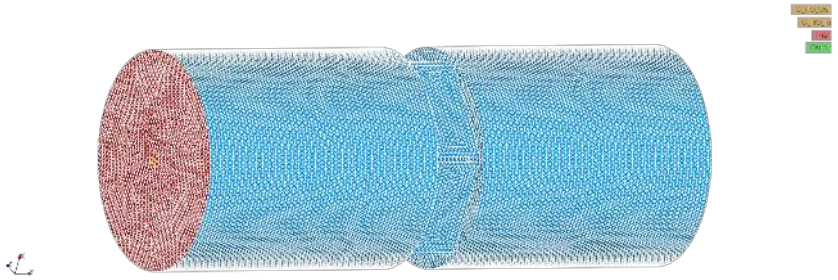

Figure 2: Finite element mesh of the acoustic media (air) volume. The plane wave inlet is on the left (indicated by red). The probe measurements are performed on the opposite (right) end of the cylindrical waveguide.

using the Python 2.7 plugin functionality for possible rapid design changes and optimizations. The Finite Element Analysis has been performed using open-source FE solver Code-Aster with pressure acoustics functionality.[16] During the simulation the Helmholtz equations are solved in frequency domain, and the entire spectrum between 300 and 1000 Hz is covered. The FE mesh is shown in Fig. 2 and consists of tetrahedral 3D elements generated by Netgen algorithm inside of SMESH plugin of Salome.

3. RESULTS AND DISCUSSION

The FE simulations in Code-Aster were performed in the frequency range 300-1000 Hz with a step size 1 Hz. A particle velocity boundary condition was applied to the inlet surface on the left side of the waveguide shown in Fig. 2. The probe measurements of the acoustic pressure amplitude were collected on the right (outlet) end of the waveguide.

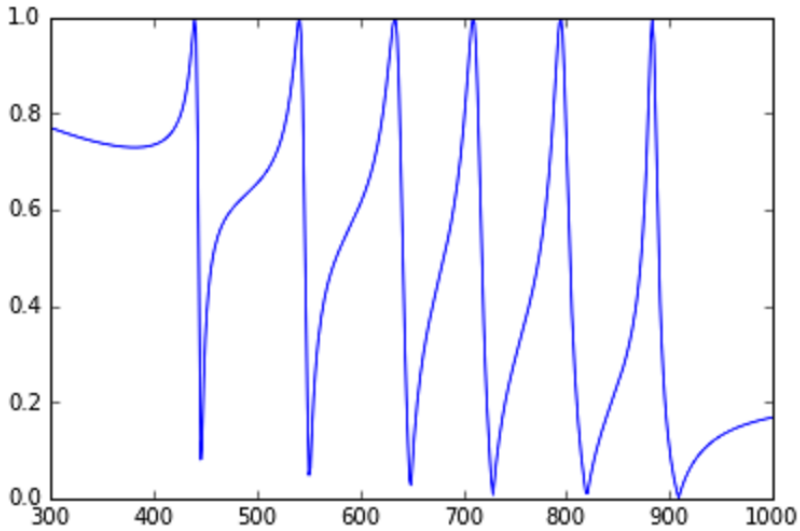

Figure 3: Frequency spectrum response of the sample hexagonal unit cell. Normalized pressure amplitude is plotted against the operational frequency.

The experimental measurements were performed in the anechoic room using a plane wave speaker, a

microphone and a 3D printed sample hexagonal cell with the corresponding six hole diameter values of 2.5, 3.2, 3.9, 4.6, 5.3 and 6.0 mm.

A. FINITE ELEMENT MODELLING RESULTS

The resulting frequency transmission spectrum is shown in Fig. 3. The measured acoustic field amplitude at the exit end of the waveguide shows a near-complete sound blocking at six frequency values corresponding to the resonant frequencies of six in-built resonators. Moreover, packing all peak frequencies in the desired noise range has produced a partial sound blocking in the entire range between 300 and 1000 Hz.

B. EXPERIMENTAL RESULTS

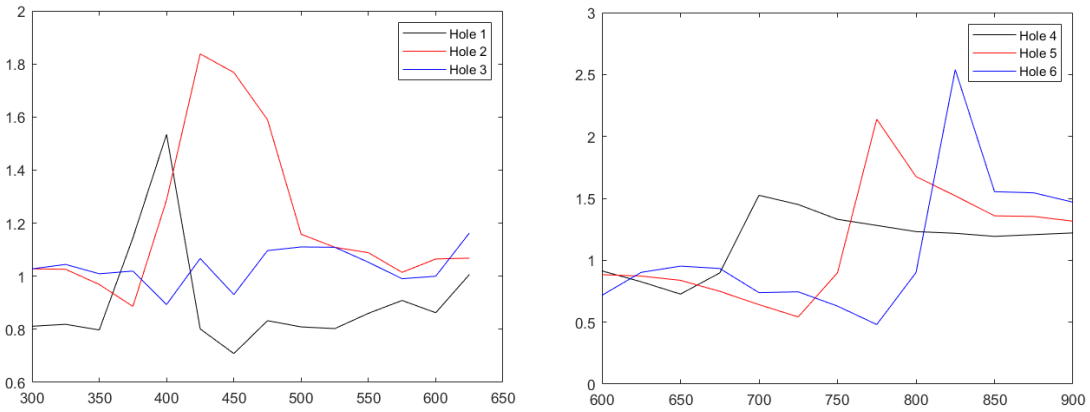

Figure 4: Normalized sound attenuation levels for six experimental runs with six independently operational resonators. (left) attenuation ratio coefficients for the three resonators with smaller hole diameters (holes 1, 2, 3). (right) the attenuation ratio for the resonators with larger holes (4, 5, 6)

.

The results of the experimental measurements are shown in Fig. 4. One sample hexagonal cell has been used with hole diameters ranging between 2.5 and 6.0 mm. The effect of each resonator on sound attenuation has been investigated separately. In order to achieve this, only one resonator hole was left open during each experimental run, while the remaining holes blocked with a duct seal. Six experimental trial runs have produced the corresponding noise attenuation spectra related to functional hole 1, hole 2, ... , hole 6. The results are showing that the resonators with smaller holes have attenuated the sound levels at lower frequencies, as expected from theory of Helmholtz resonators. The corresponding resonance frequencies, observed in the experiments and predicted by FE simulations, agree quite well with each other on average. However, we have also observed that the attenuation frequency corresponding to the resonator 2 in the experiment is lower than the one predicted from modelling by about 100 Hz. Moreover, isolated resonator 3 has failed to produce a statistically significant sound attenuation. These issues in the 500-600 Hz range are likely to be specific to the current experimental setup and will be addressed in future investigations. Nevertheless, a good agreement is still present for higher and lower frequencies.

4. CONCLUSION

A simple modular passive sound barrier has been designed and shown a good promise in noise attenuation applications while preserving a high ventilation duct surface ratio. The unit cell of the barrier wall has a hexagonal shape and contains six slightly different Helmholtz resonators built in the walls. The thickness of the barrier is in the subwavelength range and each resonator has a unique adjustable eigenfrequency, which allows to cover a customized broad range of noise levels. The design process is automated via Python scripting and is easy and cheap to manufacture for potential mass production. The attenuation frequency spectra predicted by FE modelling and observed in the anechoic room experiments are in good agreement; however, a more sensitive experimental setup is needed in future work to provide more accurate performance assessments.

ACKNOWLEDGMENTS

The authors would like to thank A-STAR for funding support under AMEIRG18-0081.

REFERENCES

[1] L. Huang, "Broadband sound reflection by plates covering side-branch cavities in a duct", *J. Acoust. Soc. Am.* **119**, 2628 (2006).

[2] C. Wang, L. Cheng, L. Huang, "Realization of a broadband low-frequency plate silencer using sandwich plates", *J. Sound Vib.* **318**, 792-808 (2008).

[3] A.Selamet, Z.L.Ji, "Acoustic attenuation performance of circular expansion chambers with extended inlet/outlet", *J. Sound Vib.* **223**, 197-212 (1999).

[4] J. W. Lee, G.-W. Jang, "Topology design of reactive mufflers for enhancing their acoustic attenuation performance and flow characteristics simultaneously", *Int. J. Numer. Methods Eng.* **91**, 552 (2012).

[5] N. Sellen, M. Cuesta, and M. Galland, "Noise reduction in a flow duct: Implementation of a hybrid passive/active solution", textslJ. Sound Vib. **297**, 492 (2006).

[6] G. W. Stewart, "The Theory of the Herschel-Quincke Tube", *Phys. Rev.* **31**, 696 (1928).

[7] S. A. Cummer, J. Christensen, A. Alu, "Controlling sound with acoustic metamaterials", *Nature Mat.*, **1**, 1-13, (2016).

[8] M. Sun, X. Fang, D. Mao, X. Wang, Y. Li, "Broadband Acoustic Ventilation Barriers", *Phys. Rev. App.*, **13**, 044028, (2020).

[9] R. Ghaffarivardavagh, J. Nikolajczyk, S. Anderson, X. Zhang, "Ultra-open acoustic metamaterial silencer based on Fano-like interference", *Phys. Rev. B*, **99**, 024302, (2019).

[10] Y. Li, B. Assouar, "Acoustic metasurface-based perfect absorber with deep subwavelength thickness", *Appl. Phys. Lett.*, **108**, 063502, (2016).

[11] H. Chang, L. Liu, C. Zhang, X. Hu, "Broadband high sound absorption from labyrinthine metasurfaces", *AIP Adv.*, **8**, 045115, (2018).

[12] J. Christensen, L. Martn-Moreno, F. J. Garcia-Vidal, "All-angle blockage of sound by an acoustic double-fishnet metamaterial", *Appl. Phys. Lett.*, **97**, 134106, (2010).

[13] J. Li, W. Wang, Y. Xie, B.-I. Popa, S. A. Cummer, "A sound absorbing metasurface with coupled resonators", *Appl. Phys. Lett.*, **109**, 091908, (2016).

[14] N. Jimnez, V. Romero-Garca, V. Pagneux, J.-P. Groby, "Rainbow-trapping absorbers: Broadband, perfect and asymmetric sound absorption by subwavelength panels for transmission problems", *Sci. Rep.*, **7**, 13595, (2017).

[15] A. Ribes, C. Caremoli, *COMPSAC 07: Proceeding of the 31st Annual International Computer Software and Applications Conference*, 553-564 (2007).

[16] EDF, "Finite element code-aster, analysis of structures and thermomechanics for studies and research", Open source on www.code-aster.org (1989-2017).